

Cyclic Donor–Acceptor Circuits: Synthesis and Fluorescence Ion Sensory Properties of a Mixed-Heterocyclic Dehydroannulene-Type Cyclophane

Paul N. W. Baxter

Institut Charles Sadron, UPR 022, 6 Rue Boussingault, F-67083 Strasbourg, France

baxter@ics.u-strasbg.fr

Received July 28, 2003

The new dehydroannulene-type cyclophane **5** comprising a conjugated helical framework of thiophene (electron donor) and pyridine (electron acceptor) heterocyclic units has been prepared. Macrocycle **5** was characterized by FAB MS and ^1H and ^{13}C NMR spectroscopy. Cycle **5** was found to function as a selective precipitation and fluorescence sensor for specific metal ions such as Ag^{\dagger} and also exhibited reversible proton-triggered fluorescence quenching behavior. The unique donor–acceptor architecture and spectroscopic properties of **5** suggest that it represents a novel lead class of molecular sensory platforms, with many potential future applications in 21st century materials science.

Introduction

Ethynyl cyclophanes currently represent a rapidly expanding class of organic high carbon content substrates that promise many interesting and novel applications within the fields of supramolecular chemistry and materials science.^{1a–f} For example, specific types of ethynyl cyclophanes have recently been discovered to exhibit potentially useful properties such as solid-state porosity,^{1a,2a–b} liquid crystallinity,^{3a–c} and energy storage capabilities,^{1e,4a–c} whereas others have been demonstrated to serve as potential starting substrates for the generation of fullerenes,^{5a–d} carbon nanotubules,^{4a} carbon networks,^{6a–d} and nanostructures.^{7a–c}

However, the majority of ethynyl macrocycles synthesized to date have been constructed from purely hydrocarbon subunits. A particularly interesting avenue of investigation would therefore be to incorporate metal-ion-binding aromatic heterocycles into the macrocyclic framework. Complexes of this type may be expected to display a rich variety of exploitable properties such as electrochemical, photochemical, magnetic, optical, catalytic, mechanical, and sensory abilities.^{8a–p}

(1) (a) Gleiter, R.; Werz, D. B.; Rausch, B. J. *Chem. Eur. J.* **2003**, *9*, 2676. (b) Grave, C.; Schlüter, A. D. *Eur. J. Org. Chem.* **2002**, 3075. (c) Kennedy, R. D.; Lloyd, D.; McNab, H. *J. Chem. Soc., Perkin Trans. 1* **2002**, 1601. (d) Diederich, F. *Chem. Commun.* **2001**, 219. For an informative series of reviews covering the field up to 1999, see: (e) *Top. Curr. Chem.* **1999**, *201*, entire volume. (f) Höger, S. *J. Polym. Sci., Part A: Polym. Chem.* **1999**, *37*, 2685.

(2) (a) Campbell, K.; Kuehl, C. J.; Ferguson, M. J.; Stang, P. J.; Tykwinski, R. R. *J. Am. Chem. Soc.* **2002**, *124*, 7266. (b) Venkataraman, D.; Lee, S.; Zhang, J.; Moore, J. S. *Nature* **1994**, *371*, 591.

(3) (a) Godt, A.; Duda, S.; Ünsal, Ö.; Thiel, J.; Härter, A.; Roos, M.; Tschierske, C.; Diele, S. *Chem. Eur. J.* **2002**, *8*, 5094. (b) Höger, S.; Enkelmann, V.; Bonrad, K.; Tschierske, C. *Angew. Chem., Int. Ed.* **2000**, *39*, 2268. (c) Zhang, J.; Moore, J. S. *J. Am. Chem. Soc.* **1994**, *116*, 2655.

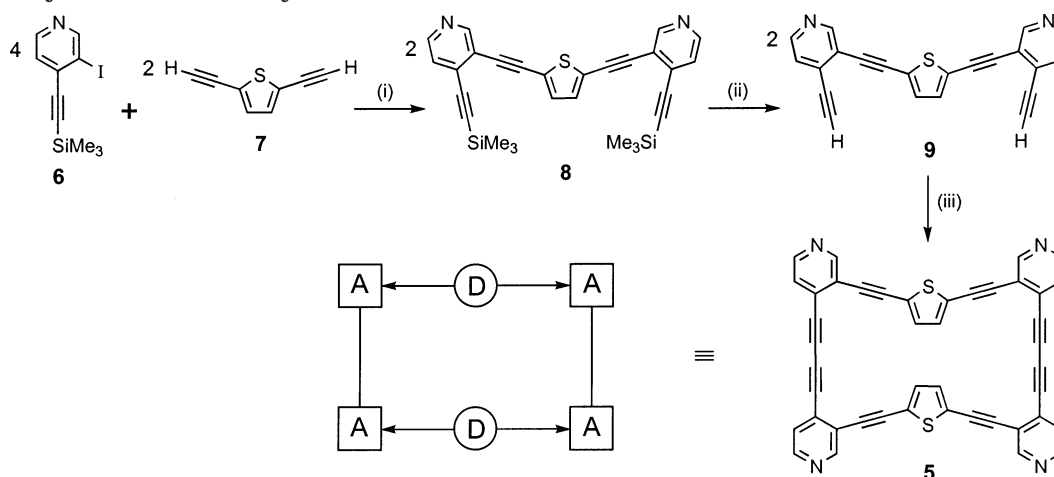
(4) (a) Boese, R.; Matzger, A. J.; Vollhardt, K. P. C. *J. Am. Chem. Soc.* **1997**, *119*, 2052. (b) de Meijere, A.; Kozhushkov, S.; Haumann, T.; Boese, R.; Puls, C.; Cooney, M. J.; Scott, L. T. *Chem. Eur. J.* **1995**, *1*, 124. (c) de Meijere, A.; Kozhushkov, S.; Puls, C.; Haumann, T.; Boese, R.; Cooney, M. J.; Scott, L. T. *Angew. Chem.* **1994**, *106*, 934; *Angew. Chem., Int. Ed. Engl.* **1994**, *33*, 869.

(5) (a) Tobe, Y.; Nakanishi, H.; Sonoda, M.; Wakabayashi, T.; Achiba, Y. *Chem. Commun.* **1999**, 1625. (b) Tobe, Y.; Nakagawa, N.; Naemura, K.; Wakabayashi, T.; Shida, T.; Achiba, Y. *J. Am. Chem. Soc.* **1998**, *120*, 4544. (c) Rubin, Y.; Parker, T. C.; Pastor, S. J.; Jalisatgi, S.; Bouille, C.; Wilkins, C. L. *Angew. Chem.* **1998**, *110*, 1353; *Angew. Chem., Int. Ed.* **1998**, *37*, 1226. (d) Rubin, Y. *Chem. Eur. J.* **1997**, *3*, 1009 and references therein.

(6) (a) Bunz, U. H. F.; Rubin, Y.; Tobe, Y. *Chem. Soc. Rev.* **1999**, *28*, 107. (b) Diederich, F. *Nature* **1994**, *369*, 199. (c) Bunz, U. H. F. *Angew. Chem.* **1994**, *106*, 1127; *Angew. Chem., Int. Ed. Engl.* **1994**, *33*, 1073. (d) Diederich, F.; Rubin, Y. *Angew. Chem.* **1992**, *104*, 1123; *Angew. Chem., Int. Ed. Engl.* **1992**, *31*, 1101.

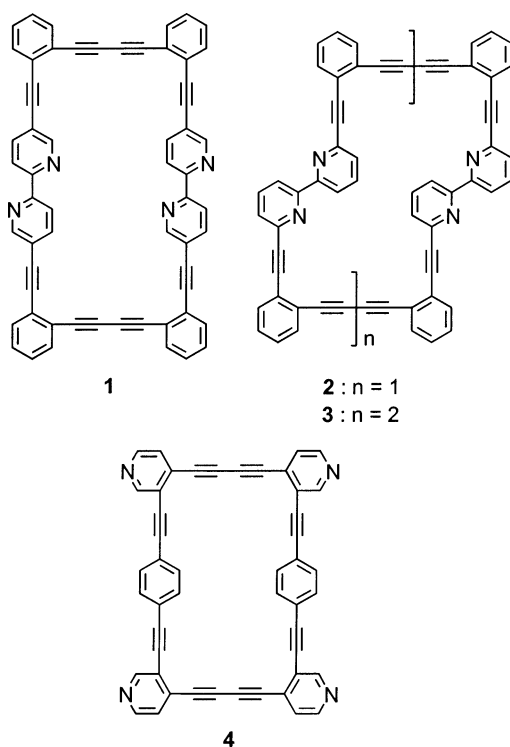
(7) (a) Mayor, M.; Didschies, C. *Angew. Chem., Int. Ed.* **2003**, *42*, 3176. (b) Mena-Osteritz, E.; Bäuerle, P. *Adv. Mater.* **2001**, *13*, 243. (c) Moore, J. S. *Acc. Chem. Res.* **1997**, *30*, 402.

(8) The construction of ethynyl macrocycles incorporating pyridine and pyridine-type heterocycles has recently been the focus of a surge in interest. For examples of conjugated ethynyl macrocycles incorporating pyridine units, see: (a) Baxter, P. N. W. *Chem. Eur. J.* **2003**, *9*, 2531. (b) Campbell, K.; McDonald, R.; Ferguson, M. J.; Tykwinski, R. R. *Organometallics* **2003**, *22*, 1353. (c) Campbell, K.; McDonald, R.; Tykwinski, R. R. *J. Org. Chem.* **2002**, *67*, 1133. (d) Campbell, K.; McDonald, R.; Branda, N. R.; Tykwinski, R. R. *Org. Lett.* **2001**, *3*, 1045. (e) Sun, S.-S.; Lees, A. J. *Organometallics* **2001**, *20*, 2353. (f) Bosch, E.; Barnes, C. L. *Organometallics* **2000**, *19*, 5522. (g) Tobe, Y.; Nagano, A.; Kawabata, K.; Sonoda, M.; Naemura, K. *Org. Lett.* **2000**, *2*, 3265. (h) Reference 5a. For examples of conjugated ethynyl macrocycles incorporating bipyridine units, see: (i) Baxter, P. N. W. *Chem. Eur. J.* **2002**, *8*, 5250. (j) Henze, O.; Lentz, D.; Schäfer, A.; Franke, P.; Schlüter, A. D. *Chem. Eur. J.* **2002**, *8*, 357. (k) Baxter, P. N. W. *J. Org. Chem.* **2001**, *66*, 4170. (l) Henze, O.; Lentz, D.; Schlüter, A. D. *Chem. Eur. J.* **2000**, *6*, 2362. (m) Henze, O.; Lehmann, U.; Schlüter, A. D. *Polym. Mater. Sci. Eng.* **1999**, *80*, 231. For ethynyl macrocycles incorporating terpyridine units, see: (n) Grave, C.; Lentz, D.; Schäfer, A.; Samorì, P.; Rabe, J. P.; Franke, P.; Schlüter, A. D. *J. Am. Chem. Soc.* **2003**, *125*, 6907. (o) Baxter, P. N. W. *Chem. Eur. J.* **2003**, *9*, 5011. For an example of a conjugated phenylethynyl macrocycle incorporating phenanthroline units, see: (p) Schmittl, M.; Ammon, H. *Synlett* **1999**, 750.

SCHEME 1. Synthesis of Macrocycle 5^a

^a (i) PdCl₂(PPh₃)₂, CuI cat., toluene, Et₃N, 20 °C, 5 d (54%); (ii) 1 M (^tBu)₄NF, THF, H₂O, 20 °C, 20 h (88%); (iii) [Cu₂(OAc)₄]2H₂O, pyridine, 20 °C, 7 d (46%).

Earlier investigations into the abovementioned possibilities focused upon the synthesis of bipyrido- and pyrido-dehydroannulene-type structures 1–4. As anti-



pated, the latter macrocycles were found to be strongly fluorescent chromophores affording characteristic fluorescence sensory output responses in the presence of particular metal ions. Thus, 1 was found to be a selective chromogenic sensor for Zn^{II}. Ligands 2 and 3 functioned as fluorescence sensors for Cu^{II} ions, and 4 underwent fluorescence quenching specific to the presence of Hg^{II} and Pd^{II}.^{8a,i,k}

As a first step toward controllably modifying and optimizing the physicochemical properties of 1–4, analogue 5 was prepared, in which the phenyl rings of 4 have been replaced by thiophene heterocycles (Scheme 1).

Cycle 5 is structurally unique in that it comprises comparatively electron-rich heterocycles (thiophene units), in direct electronic communication with comparatively electron-deficient heterocycles (pyridine units). A conjugated donor–acceptor cyclophane of this type would thus be expected to spectroscopically signal the presence of metal ions at significantly longer wavelengths and may potentially function as an ion sensor with enhanced visible chromogenic properties.⁹

The following report describes the successful preparation of 5 and a detailed spectroscopic investigation into its ion-binding and sensory behavior. The latter studies revealed that the UV–visible absorbances and fluores-

(9) Ethynyl-bridged pyridyl-thiophene scaffolds are attracting an increasing amount of attention due to their interesting physicochemical properties. For example, several donor–acceptor polymeric systems have been synthesized and studied with respect to their electrochemical, fluorescence, and NLO properties; see: (a) Yamamoto, T.; Honda, K.; Ooba, N.; Tomaru, S. *Macromolecules* **1998**, *31*, 7. (b) Oba, N.; Kaino, T.; Tomaru, A. Patent JP8220574, 1996. (c) Yamamoto, T.; Yamada, W.; Takagi, M.; Kizu, K.; Maruyama, T.; Ooba, N.; Tomaru, S.; Kurihara, T.; Kaino, T.; Kubota, K. *Macromolecules* **1994**, *27*, 6620. (d) Takagi, M.; Kizu, K.; Miyazaki, Y.; Maruyama, T.; Kubota, K.; Yamamoto, T. *Chem. Lett.* **1993**, 913. (e) Yamamoto, T.; Takagi, M.; Kizu, K.; Maruyama, T.; Kubota, K.; Kanbara, H.; Kurihara, T.; Kaino, T. *Chem. Commun.* **1993**, 797. Oligomeric systems have also been investigated. For electrochemical studies, see: (f) Chapman, G. M.; Stanforth, S. P.; Berridge, R.; Pozo-Gonzalo, C.; Skabara, P. J. *J. Mater. Chem.* **2002**, *12*, 2292. For the construction of organometallic end-capped NLO chains and as a precursor for the generation of second order NLO polymers, see: (g) Wu, I.-Y.; Lin, J. T.; Luo, J.; Li, C.-S.; Tsai, C.; Wen, Y. S.; Hsu, C.-C.; Yeh, F.-F.; Liou, S. *Organometallics* **1998**, *17*, 2188. (h) Reinhardt, B. A.; Kannan, R.; Bhatt, J. C.; Zieba, J.; Prasad, P. N. *Polym. Prepr. Am. Chem. Soc. Div. Polym. Chem.* **1994**, *35*, 166. The syntheses, photophysics, and electron-transfer reactivity of ethynylthienyl oligomers incorporating bipyridine and terpyridine metal complexes have recently been reported, with the goal of developing new types of electroactive molecular wires: (i) Liu, Y.; De Nicola, A.; Reiff, O.; Ziessel, R.; Schanze, K. S. *J. Phys. Chem. A* **2003**, *107*, 3476. (j) Ringenbach, C.; De Nicola, A.; Ziessel, R. *J. Org. Chem.* **2003**, *68*, 4708. (k) De Nicola, A.; Liu, Y.; Schanze, K. S.; Ziessel, R. *Chem. Commun.* **2003**, 288. (l) De Nicola, A.; Ringenbach, C.; Ziessel, R. *Tetrahedron Lett.* **2003**, *44*, 183. (m) Harriman, A.; Mayeux, A.; De Nicola, A.; Ziessel, R. *Phys. Chem. Chem. Phys.* **2002**, *4*, 2229. Related oligomeric ligands have been demonstrated to exhibit ion-modulated redox switching and to undergo metal-induced autoassembly to give supramolecular metallocycles: (n) Büschel, M.; Helldobler, M.; Daub, J. *Chem. Commun.* **2002**, 1338. (o) Sun, S.-S.; Lees, A. J. *J. Am. Chem. Soc.* **2000**, *122*, 8956. Certain small molecules incorporating the (2-thienyl)-(3-pyridyl)-ethyne moiety have also been discovered to be biologically active, serving as metalloproteinase-inhibiting agents: (p) Tucker, H.; Finlay, R.; Waterson, D. Patent WO03014111, 2003.

cence emission of **5**, as well as its spectroscopic responses to metal ions and protons, occurred at significantly lower energies compared to **4**. Cycle **5** also provided a particularly distinctive visible chromogenic fluorescence-precipitation sensory output for Ag⁺ ions.

Results and Discussion

Synthesis of 5. Cyclophane **5** was prepared using a six-step synthesis in 12% overall yield starting from 3-bromopyridine, and at a later stage in the preparation, 2,5-diethynylthiophene **7**¹⁰ (Scheme 1). The former starting material was converted to **6** as previously described.^{8a} A Sonogashira reaction¹¹ between 2 equiv of **6** and **7** in 14% Et₃N/toluene with PdCl₂(PPh₃)₂ catalyst and CuI cocatalyst afforded **8** in 54% yield after workup. Compound **8** was then desilylated with TBAF in aqueous THF to furnish the heat- and light-sensitive dialkyne **9** in 88% isolated yield. Dialkyne **9** was then finally cyclized using the Eglinton/Galbraith ethyne coupling protocol under medium/high dilution conditions in degassed pyridine with an excess of Cu₂(OAc)₄ to afford **5** in 46% yield after purification as a bright yellow solid.¹²

Characterization and Properties of 5. The structure of the product isolated from the Cu₂(OAc)₄-mediated coupling of **9** was established to be that of the macrocyclic architecture **5** (Scheme 1) on the basis of mass spectroscopic, infrared, and ¹H and ¹³C NMR spectroscopic studies.

The FAB mass spectrum of the coupling product recorded in CF₃COOH displayed a single isotope cluster peak at *m/z* = 665, corresponding exactly to that calculated for the [M⁺ + H] isotopic envelope of macrocycle **5**. This structural assignment was further substantiated by a high-resolution FAB mass spectroscopic measurement of the [M⁺ + H] isotopic envelope, which confirmed the exact elemental composition of the product to be C₄₄H₁₇N₄S₂, in accordance with the macrocyclic structure **5** plus one hydrogen.

The infrared spectrum of the coupling product of **9** was also supportive of the macrocyclic structural assignment of **5**, in that vibrational modes characteristic of the H–C≡ stretch of terminal alkynes were absent. This result establishes that the coupling product is in fact macrocyclic and not a linear oligomer with unreacted terminal ethyne groups.

The ¹³C NMR spectrum of the coupling product of **9** comprised 11 peaks, consistent with the above macrocyclic structural assignment (Figure 1). The chemical shifts of the four peaks in the range 90.3–80.6 ppm correspond to the chemically and magnetically inequivalent carbons of two unsymmetrically substituted alkyne groups, and the remaining seven correspond to the inequivalent carbons of the heterocycles.

The ¹H NMR spectrum of the coupling product of **9** displayed four resonances expected for the macrocyclic structure **5** (Figure 1). A ¹H–¹H COSY measurement verified that it was a single compound and not a mixture

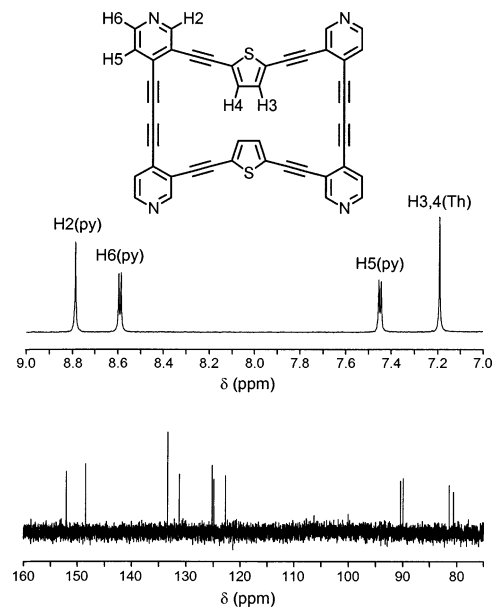


FIGURE 1. 500-MHz ¹H (upper) and 125.8-MHz ¹³C (lower) NMR spectra of **5**, recorded in CDCl₂CDCl₂ solution at 90 °C.

of species. Peaks originating from the protons of terminal ethynes were completely absent in the ¹H NMR spectrum of the coupling product, lending further support for the macrocyclic identity of this compound. Spectral assignments were made on the basis of coupling constants and comparisons with the spectra of **8** and **9**. The singlet at 8.785 ppm and the doublet at 8.591 ppm were the furthest downfield resonances in the ¹H NMR spectrum of **5**. They were therefore assigned to the pyridyl H2 and H6 protons, respectively, because of their proximity to the electron-withdrawing pyridine nitrogen. The upfield doublet at 7.451 ppm was thus assigned to the remaining pyridyl H5 proton. The singlet at 7.191 ppm due to the bridging thiophene ring protons of **5** was slightly upfield-shifted compared to those of **8** and **9** by $\Delta\delta$ = 0.092 and 0.112 ppm, respectively. On the other hand, the pyridine protons of **5** are all situated slightly downfield compared to the corresponding protons of **8** and **9**.¹³

A semiempirical AM1 molecular modeling calculation performed upon the structure assigned to **5** showed the ground state conformation to be a helically twisted macrocycle, with the thiophene sulfurs facing each other and pointing toward the center of the cycle (Figure 2). The hinged nature of the molecule allows some conformational flexibility and variation in the intrathiophene distance.

Unlike **4**, cycle **5** was found to be poorly soluble in most organic solvents, suggesting the presence of enhanced solid-state intermolecular π – π interactions in the latter compound. Cyclophane **5** was also rather light-sensitive both in solution and the solid state, rapidly darkening

(13) Inspection of molecular models of **5** show that the sulphur atoms point towards the interior of the macrocycle, and the thiophene hydrogens are situated on the outer surface of the ring in its most stable conformation. Significant structural reorganizations are required in order to orient the thiophene hydrogens toward the interior of the cycle. The fact that the thiophene protons in the ¹H NMR of **5** are only slightly shifted with respect to those of the precursors **8** and **9** supports the conclusion that they do not reside for any significant time within the macrocyclic cavity.

(10) Neenan, T. X.; Whitesides, G. M. *J. Org. Chem.* **1988**, *53*, 2489.

(11) Sonogashira, K.; Tohda, Y.; Hagihara, N. *Tetrahedron Lett.* **1975**, 4467.

(12) The Eglinton/Galbraith ethyne coupling protocol has been widely employed for macrocyclisation reactions; see for example: Rossa, L.; Vögtle, F. *Top. Curr. Chem.* **1983**, *113*, pp 72–75.

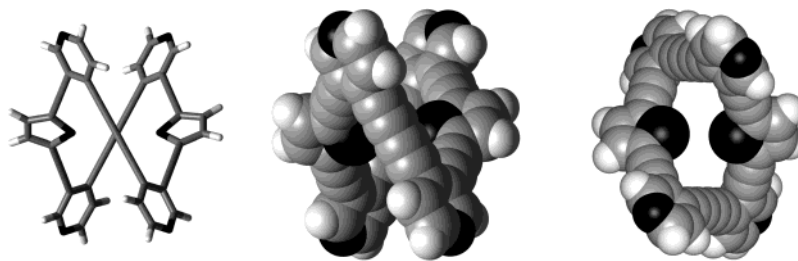


FIGURE 2. Energy minimized structure of macrocycle **5**. Left: plan view (stick representation). Center: plan view (CPK representation). Right: view through central macrocyclic cavity. The minimization was obtained by an AM1 semiempirical calculation using SPARTAN 02 Linux/Unix (Wavefunction, Inc., Irvine, CA).

in color upon exposure to direct light. Interestingly, **5** possesses thermal properties similar to those of **4**, igniting explosively when rapidly heated at ≥ 294 °C to give a black soot. Macrocycle **5** is therefore a high energy material. Thermal behavior of this type is unusual but has been observed, for example, with a dehydrotetrabenzoannulene^{4a} and a family of spiro-linked [7]-rotanes.^{4b,c}

UV–Visible Spectroscopic Sensing of Metal Ions by 5. To determine the potential viability of **5** for the chromogenic sensing of metal ions, a detailed spectroscopic investigation into its cation-binding properties was undertaken.

The UV–visible spectra of uncomplexed **5** in CHCl₃ and 10% MeOH/CHCl₃ solutions exhibit four absorbances that are invariant in energy and shape below $[5] = 5 \times 10^{-5}$ mol dm⁻³, showing that aggregation is not occurring in dilute solution. The electronic effect of the thiophene rings was clearly evident in the UV–visible spectrum of **5**, as all absorbances were shifted by 9–18 nm to lower energy compared to the spectrum of **4**.^{8a}

UV–visible spectra of **5/Mⁿ⁺** mixtures at a 1:4 stoichiometric ratio in 10% MeOH/CHCl₃ were then recorded, with $[5] = 9.63 \times 10^{-6}$ mol dm⁻³ and $M^{n+} = \text{Li}^I, \text{Na}^I, \text{K}^I, \text{Mg}^{II}, \text{Ca}^{II}, \text{Cr}^{III}, \text{Mn}^{II}, \text{Fe}^{II}, \text{Pt}^{II}, \text{Au}^I, \text{Cu}^I, \text{Cu}^{II}, \text{Zn}^{II}, \text{Cd}^{II}, \text{Pb}^{II}, \text{Tl}^I, \text{Al}^{III}, \text{In}^{III}, \text{Sc}^{III}, \text{Y}^{III}, \text{La}^{III}, \text{Eu}^{III}, \text{and Tb}^{III}$.¹⁵ All spectra showed zero or minimal changes compared to the UV–visible spectrum of **5**, indicating insignificant binding of the macrocycle to the above cations in dilute solution. However, the UV–visible spectra of **5/Hg^{II}** and **5/Pd^{II}** at a 1:4 stoichiometric ratio in 10% MeOH/CHCl₃, with $[5] = 9.63 \times 10^{-6}$ mol dm⁻³, were significantly

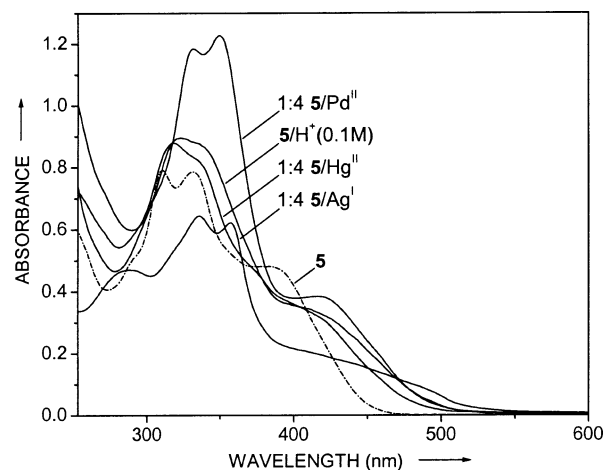


FIGURE 3. UV–vis absorption spectra of **5/Mⁿ⁺** at 1:4 stoichiometry in 10% MeOH/CHCl₃, with $M^{n+} = \text{Hg}^{II}, \text{Pd}^{II}, \text{and Ag}^I$. The **5/H⁺** spectrum was recorded in CHCl₃, 0.1 mol dm⁻³ in CF₃COOH; $[5] = 9.63 \times 10^{-6}$ mol dm⁻³ in all cases.

different from the spectrum of **5** itself, demonstrating that coordination of these ions was occurring (Figure 3). In particular, Pd^{II} caused a large increase in intensity and a concomitant shift to longer wavelengths of the free-ligand absorbances of **5**.

Similarly to **4**, when **5/Mⁿ⁺** mixtures at a 1:4 stoichiometry in 10% MeOH/CHCl₃ were prepared, with $M^{n+} = \text{Co}^{II}, \text{Ni}^{II}$ and Ag^I and $[5] = 9.63 \times 10^{-6}$ mol dm⁻³, yellow precipitates slowly developed upon standing. The precipitates formed within 1 h in the case of Co^{II} and Ni^{II} and 5 min with Ag^I. Addition of a few drops of a saturated 10% H₂O/MeOH solution of KCN to the **5/Ag^I** mixture caused complete disappearance of the precipitate and regeneration of the original UV–visible spectrum of **5**. This latter observation demonstrated that the suspended solid was a coordination polymer and not the product of an irreversible chemical reaction. A UV–visible spectrum of the **5/Ag^I** suspension comprised three clear absorbances at 287, 335, and 357 nm and a broad shoulder between 400 and 500 nm (Figure 3). The two most intense absorbance envelopes at 335 and 357 nm were shifted to a significantly lower energy compared to the spectra of the free ligand and the **5/Pd^{II}** system.

To assess the effect of interference between mixtures of ions on the binding and ultimately the potential utility of **5** as a sensor, UV–visible competition experiments were investigated with 1:4:4 mixtures of **5/M1ⁿ⁺/M2ⁿ⁺** in 10% MeOH/CHCl₃, where $[5] = 9.63 \times 10^{-6}$ mol dm⁻³ and $M1^{n+}$ and $M2^{n+} = \text{Ag}^I, \text{Hg}^{II}, \text{Co}^{II}, \text{Ni}^{II}, \text{and Pd}^{II}$. From

(14) The 1:4 stoichiometric reaction between **4** and Fe^{II} under dilute conditions resulted in the slow precipitation of a coordination polymer. No precipitation phenomena were observed during the same reaction between **5** and Fe^{II}. A partial reduction in the intensity of the absorbance of the mixture did occur upon standing for 48 h, indicating the development of a slight interaction between **5** and Fe^{II} over prolonged periods of time. However, the visual fluorescence of the mixture remained unchanged. Cycle **4** therefore appears to exhibit a much stronger interaction with Fe^{II} compared to **5**.

(15) The metal chlorides and complexes used in the study were CrCl₃·6H₂O, FeCl₂, CoCl₂·6H₂O, NiCl₂·6H₂O, PdCl₂(MeCN)₂, PtCl₂(MeCN)₂, [Cu(MeCN)₄]BF₄, and AuCl(THT). All remaining cations investigated were in the form of their anhydrous triflates. With the exception of PdCl₂(MeCN)₂, [Cu(MeCN)₄]BF₄, and AuCl(THT), all solutions were prepared in MeOH. The chromium, iron, cobalt, and nickel chlorides were each dissolved in a drop of distilled water prior to the preparation of the standard solutions in methanol to ensure complete solubility. For the same reason, the palladium and platinum complexes were initially dissolved in 1 mL of warm acetonitrile and in the former case diluted to the required volume with CH₂Cl₂. The AuCl(THT) solution was prepared in CH₂Cl₂, and the [Cu(MeCN)₄]BF₄ solution in MeCN. The Hg(CF₃SO₃)₂ was prepared from the reaction between HgO and (CF₃SO₂)₂O.^{8a} The Cu^{II}, Ag^I, and Tl^I triflates used were $\geq 99.9\%$ purity.

TABLE 1. Variation in Emission Energies of **4** and **5** with Solvent Polarity

entry	solvent ^a	λ_{\max} (nm) ^b	
		4	5
1	toluene	431, 454	479
2	CHCl ₃	436sh, 454	485
3	CH ₂ Cl ₂	440sh, ^c 453	488
4	10% MeOH/CHCl ₃	440sh, ^c 455	490
5	50% MeOH/CHCl ₃	455	495
6	10% CHCl ₃ /DMF	452	497
7	10% CHCl ₃ /DMSO	454	499

^a The Dimroth and Reichardt $E_T(30)$ solvent polarity indices are as follows: MeOH (55.4), DMSO (45.1), DMF (43.2), CH₂Cl₂ (40.7), CHCl₃ (39.1), and toluene (33.9). ^b [**4**], [**5**], and λ_{ex} were, respectively, 8.58×10^{-6} mol dm⁻³ (301 nm) and 9.63×10^{-6} mol dm⁻³ (332 nm). ^c The fluorescence emission envelopes at 453 and 455 nm (entries 3 and 4) are asymmetric in shape, with an incipient shoulder at 440 nm.

these latter studies and from characteristic visual fluorescence responses (see below), the overall ion-binding preference of **5** was found to occur in the following qualitative order, Pd^{II} >> Ni^{II} > Co^{II} > Ag^I > Hg^{II}. Thus the presence of Pd^{II} with Ni^{II}, Co^{II}, and Ag^I suppressed precipitation in all three cases.

Fluorescence Emission Properties of 5. Solutions of **5** in organic solvents emit a turquoise fluorescence when irradiated with UV light. The fluorescence emission of **5** in aerated and deoxygenated CHCl₃ solution comprised a single maximum at 485 nm when excited at the wavelength of the absorption envelope at 332 nm. The excited state of **5** is therefore insensitive to quenching by oxygen. The energy of the emission maximum remained unchanged at concentrations below 4×10^{-5} mol dm⁻³, showing that aggregation of the excited state was not occurring in dilute solution. Furthermore, the fluorescence emission of **5** occurred at 31 nm lower energy compared to that of **4** in CHCl₃ solution (Table 1), illustrating the enhanced intramolecular donor–acceptor nature of the excited state of **5**. The fluorescence of **5** is also significantly lower in energy compared to that of precursors **8** and **9**, exemplifying the increased conjugation of the macrocyclic ring (Table 1, Figure 4).

Interestingly, changing the solvent to 10% MeOH/CHCl₃ caused a small decrease in the emission energy of **5** to 490 nm. A more detailed investigation into the latter effect revealed that the fluorescence emission of **5** was positively solvatochromic, shifting to lower energies upon increasing solvent polarity (Table 1).¹⁶ The emission wavelength of **5** increased by 20 nm on changing the solvent from toluene to 10% CHCl₃/DMSO. This result is consistent with the equilibrium (solvent relaxed) excited state of **5** possessing a much greater polarity than the ground state. Polar solvents would be expected to stabilize the latter excited state and destabilize the Franck–Condon ground state relative to the equilibrium ground state by differential solvation. By contrast, the emission of **4** was mostly insensitive to the nature of the solvent medium (Table 1). Interestingly, however, **4** showed an additional distinct emission at 431 nm in toluene, in addition to the solvent-insensitive band at 454

(16) The solvent polarity used in this context is defined by the $E_T(30)$ scale of Dimroth and Reichardt. For a comprehensive review on this subject, see: Reichardt, C. *Chem. Rev.* **1994**, *94*, 2319.

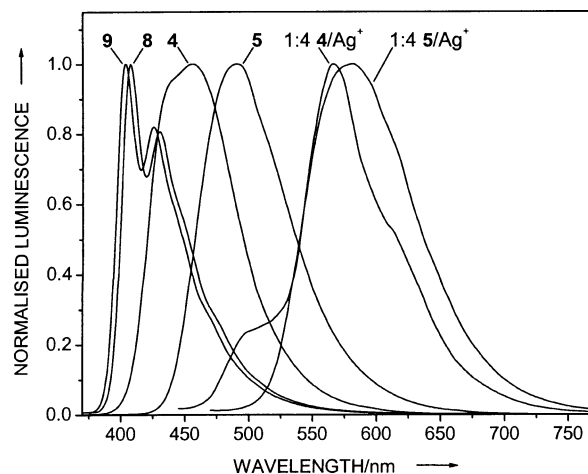


FIGURE 4. Normalized fluorescence emission spectra of **4** and **5** in 10% MeOH/CHCl₃, **8** and **9** in CHCl₃ solution [at concentrations, mol dm⁻³ (λ_{ex} , nm) of, respectively: 8.58×10^{-6} (301), 9.63×10^{-6} (332), 3.34×10^{-6} (371) and 4.07×10^{-6} (367)], and luminescence spectra of 1:4 **4**/Ag⁺ and 1:4 **5**/Ag⁺ [recorded as suspensions in 10% MeOH/CHCl₃, where [**4**] = 8.58×10^{-6} mol dm⁻³ (λ_{ex} = 405 nm) and [**5**] = 9.63×10^{-6} mol dm⁻³ (λ_{ex} = 400 nm)].

nm. The 431 nm emission appeared to be slightly positively solvatochromic and merged into the solvent-insensitive envelope upon increase of the medium polarity.¹⁷

Luminescence Sensing of Metal Ions by 5. The fluorescence emission behavior of the 1:4 stoichiometric solutions of **5**/Mⁿ⁺ in 10% MeOH/CHCl₃ was then investigated, where [**5**] = 9.63×10^{-6} mol dm⁻³ and Mⁿ⁺ = all cations and metal chlorides investigated in the UV–visible spectroscopic studies described above.

Fluorescence changes were qualitatively observed only in the cases of Ag^I, Co^{II}, Ni^{II}, and Pd^{II}. Specifically, the **5**/Co^{II} mixture displayed partial fluorescence quenching 2–3 h after mixing. After 24 h, however, the fluorescence had returned and was of the same color as that of the uncomplexed ligand. The **5**/Mⁿ⁺ (Mⁿ⁺ = Ni^{II}, Pd^{II}) reactions were accompanied by complete visual fluorescence quenching shortly after addition of the metal salt. By contrast, the precipitate that developed in the **5**/Ag⁺ reaction exhibited a characteristic bright orange luminescence at 581 nm when excited at 400 nm. The precipitate that formed in the **4**/Ag⁺ reaction was also luminescent when excited at similar wavelengths, but the color was pale yellow, reflecting the overall higher energy emission of **4** compared to that of **5** (Figure 4).¹⁸ Unlike the previously studied **4**/Hg^{II} system, the **5**/Hg^{II} reaction gave zero fluorescence response, even after

(17) Cycles **4** and **5** were found to exhibit limited ambient temperature solubility in particular solvents and especially those of high polarity. To obtain reproducible results, the solutions of **4** and **5** in CH₂Cl₂ were briefly refluxed and then allowed to cool to ambient temperature before final dilution to the required solution volume of 5 mL. For the same reasons, **4** and **5** were prepared as 10% CHCl₃ solutions in DMF and DMSO and 50% MeOH in CHCl₃ to ensure complete dissolution. Zero change in the emission spectrum of the toluene solution of **4** occurred upon further dilution, consistent with a solvatochromic rather than aggregation-induced origin of the higher energy 431 nm emission. It may finally be noted that the emission of **4** at 453 nm in CH₂Cl₂ solution, erroneously reported in ref 8a as being corrected for the instrumental response, was in fact uncorrected for the instrumental response.

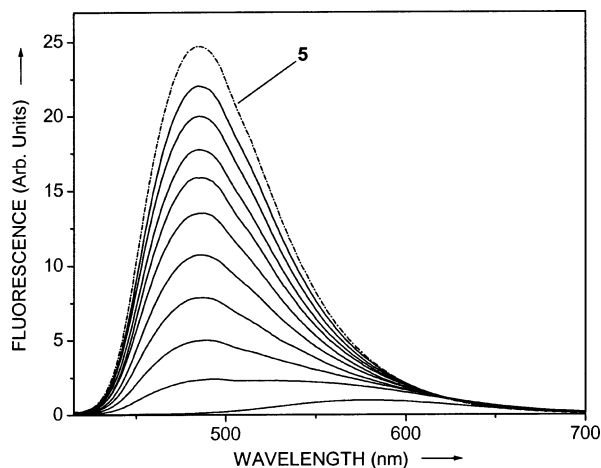


FIGURE 5. Fluorescence emission spectra of **5** with incremental additions of CF_3COOH at $[\mathbf{5}] = 1.93 \times 10^{-6} \text{ mol dm}^{-3}$ in CHCl_3 , and $[\text{H}^+]$ of, respectively, 1.0, 1.2, 1.3, 1.4, 1.5, 1.75×10^{-3} ; 1.0, 1.2, 1.3×10^{-2} ; and $1.0 \times 10^{-1} \text{ mol dm}^{-3}$ ($\lambda_{\text{ex}} = 400 \text{ nm}$).

standing for 24 h. This result is somewhat surprising considering the structural similarity of **4** and **5**.

Proton-Modulated Fluorescence of 5. The fluorescence intensity of **5** is also sensitive to the presence of protons. In a qualitative investigation of this process, CF_3COOH was titrated into a $1.93 \times 10^{-6} \text{ mol dm}^{-3}$ solution of **5** in CHCl_3 solution, and the fluorescence emission spectral changes were recorded (Figure 5). The fluorescence emission spectra of the **5**/ H^+ solutions exhibited strong proton-induced quenching in the fluorescence of **5** as $[\text{H}^+]$ was increased, with almost total extinction of the original emission maximum at $[\text{H}^+] > 0.1 \text{ mol dm}^{-3}$. A low intensity emission envelope at 580 nm also developed at high $[\text{H}^+]$. Extraction of the solution of **5**, where $[\text{H}^+] = 0.1 \text{ mol dm}^{-3}$, with aqueous NaOH caused complete regeneration of the original unprotonated spectrum of the macrocycle. This demonstrates that the CF_3COOH -initiated fluorescence changes in **5** were due to reversible acid–base equilibria and not irreversible chemical reactions.^{19a–d}

(18) The precipitate that formed upon the 1:4 stoichiometric reaction of **4** and **5** with $\text{Ag}(\text{CF}_3\text{SO}_3)$ in 10% $\text{MeOH}/\text{CHCl}_3$ is almost certainly an insoluble coordination polymer that may be a branched or network structure. The solid is, however, rather fragile as ultrasonication of the reaction mixtures results in redissolution of the suspensions and regeneration of the original free-ligand fluorescence, indicating that the polymers have been destroyed. Conjugated luminescent coordination oligomers and polymers are particularly interesting with respect to materials science applications as they may potentially function as energy transfer relays in photonic devices and as hybrid electroluminescent LEDs. For examples of luminescent Ag^I coordination polymers with pyridyl and imine-type ligands, see: (a) Seward, C.; Chan, J.; Song, D.; Wang, S. *Inorg. Chem.* **2003**, *42*, 1112. (b) Tong, M.-L.; Shi, J.-X.; Chen, X.-M. *New J. Chem.* **2002**, *26*, 814. (c) Tong, M.-L.; Chen, X.-M.; Ye, B.-H.; Ji, L.-N. *Angew. Chem., Int. Ed.* **1999**, *38*, 2237.

(19) Proton-controllable fluorescence phenomena have been reported for oligomeric linear, branched, and cyclic conjugated organic scaffolds incorporating nitrogen-donor heterocycles; see: (a) References 8a,i. (b) Martin, R. E.; Wytko, J. A.; Diederich, F.; Boudon, C.; Gisselbrecht, J.-P.; Gross, M. *Helv. Chim. Acta* **1999**, *82*, 1470. (c) Pabst, G. R.; Pfüller, O. C.; Sauer, J. *Tetrahedron* **1999**, *55*, 5047. (d) Yamamoto, T.; Sugiyama, K.; Kushida, T.; Inoue, T.; Kanbara, T. *J. Am. Chem. Soc.* **1996**, *118*, 3930. Macrocycle **5** and related structures are thus promising candidates for the construction of proton switches, transducers, and conductors, as well as pH-responsive NLO and electroluminescent materials.

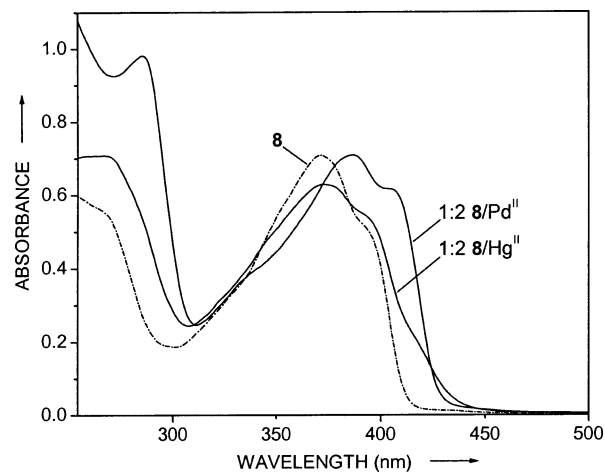


FIGURE 6. UV–vis absorption spectra of 1:2 **8**/ M^{n+} solutions in 10% $\text{MeOH}/\text{CHCl}_3$, where $M^{n+} = \text{Hg}^{\text{II}}$ and Pd^{II} at $[\mathbf{8}] = 2.01 \times 10^{-5} \text{ mol dm}^{-3}$. The spectra were recorded within 10 min from mixing.

The **5**/ CF_3COOH fluorescence quenching pH titration curve including all data points exhibited two protonation domains at $[\text{H}^+]$ in the ranges 1×10^{-3} to 8×10^{-3} and 1.3×10^{-2} to $4 \times 10^{-2} \text{ mol dm}^{-3}$. Interestingly, the proton-induced fluorescence changes in **5** were virtually identical to those of a related titration of CF_3COOH into CHCl_3 solutions of **4**. The latter result demonstrates that the pyridine nitrogen basicities of the excited states of both **4** and **5** are essentially the same and therefore insensitive to the intramolecular donor–acceptor transition.²⁰

Spectroscopic Metal Ion Sensing by Precursor **8**.

A comparative spectroscopic investigation into the metal-ion-binding properties of acyclic precursor **8** was also undertaken in order to determine the effect of macrocyclic conjugation on the complexation and sensory abilities of **5**. The UV–visible spectrum of **8** is simpler than that of **5**, comprising two bands at, respectively, 371 nm and a shoulder at 391 nm in CHCl_3 and 10% $\text{MeOH}/\text{CHCl}_3$ (Figure 6). Ligand **8** also emitted a purple-blue fluorescence when excited with a lamp operating at 365 nm, and its fluorescence spectrum comprised two sharp emissions at 407 and 430 nm, respectively (Figure 4).

The metal-ion-binding experiments were conducted with **8**/ M^{n+} at a 1:2 stoichiometry in 10% $\text{MeOH}/\text{CHCl}_3$ where $[\mathbf{8}] = 2.01 \times 10^{-5} \text{ mol dm}^{-3}$ and $M^{n+} =$ all cations and metal chlorides investigated in the spectroscopic studies of **5** above. No metal-ion-induced precipitation phenomena were observed for any **8**/ M^{n+} mixture. In addition, the **8**/ M^{n+} combinations where $M^{n+} = \text{Ag}^I$, Co^{II} , and Ni^{II} showed negligible or zero UV–visible and fluorescence spectroscopic changes, indicating either very weak or no binding of **8** to these metal ions. Similarly to **5**, the addition of Pd^{II} engendered significant changes in the UV–visible spectrum of **8** (Figure 6), which comprised a shifting of the free ligand absorbance band and shoulder to lower energy and an accompanying intensifying of the yellow coloration of the reaction solution. The

(20) This is consistent with an attenuation in electronic communication between the pyridine nitrogen and the phenyl and thiophene rings in **4** and **5** due to their *meta*-connectivity and the intramolecular donor–acceptor interaction in **5** involving predominantly π -type orbitals.

addition of Pd^{II} also caused complete fluorescence quenching of **8**. The UV–visible spectrum of **8** was also sensitive to the presence of Hg^{II} (Figure 6) and underwent slow time-dependent changes during the first 24 h after mixing. With the exception of Pd^{II}, all other metals investigated had a zero effect upon the fluorescence of **8**.

Interestingly and similarly to **4**, the UV–visible spectrum of ligand **8** experienced slight changes in the presence of Sc^{III}, In^{III}, Al^{III}, and Cr^{III}, suggesting the existence of weak binding interactions. Of all metal ions and chlorides investigated, only PdCl₂ induces a fluorescence response with **8**. Precursor **8** may therefore be considered as a highly specific fluorescence sensor for the latter metal.

Conclusion

The above work describes the preparation and spectroscopic characterization of twistophane **5**, which to the best of the author's knowledge is the first reported example of a dehydroannulene-type cyclophane incorporating both donor and acceptor heterocycles into the conjugated macrocyclic framework.²¹ Cycle **5** comprises the following structural features: (i) cyclic *ortho*-conjugation, (ii) chirality, (iii) sites for the coordination of metal ions, and (iv) intramolecular electronic donor–acceptor dipoles. These characteristics collectively support the conclusion that **5** represents a structurally unique ligand scaffold that should possess novel physicochemical properties. Investigations into the metal-binding profile of **5** demonstrated that the macrocycle functions as particularly specific sensor for Ag^I ions, exhibiting a highly characteristic chromogenic fluorescence/precipitation output response for this ion.²² The strong binding preference of **5** for Ni^{II} suggests that the latter cycle and related systems may potentially function as fluorescence quenching/precipitation sensors for Ni^{II} in biological media. Interestingly, **5** also undergoes proton-triggered fluorescence quenching, suggesting that it may potentially function as a component of a molecular logic circuit.²³

Twistophane **5** represents a structurally and electronically unique conjugated ligand.²⁴ It may therefore offer significant future potential in the design and construction

of molecular sensors,²⁵ coordination polymers,²⁶ and metal-assembled nanoarchitectures²⁷ with novel electronic²⁸ and magnetic properties, as well as the development of proton/metallo-tunable nonlinear optical (NLO) materials²⁹ and organic light-emitting diodes (OLEDs).³⁰ The preparation of elongated helical analogues of **5**, libraries of dehydroannulene-architectures with varying heterocyclic donor/acceptor combinations, and studies of their NLO and metal coordination properties will be reported.

Experimental Section

General. Standard inert atmosphere and Schlenk techniques were employed for reactions conducted under argon. Starting materials **6**^{8a} and **7**¹⁰ were prepared as described. The catalysts PdCl₂(PPh₃)₂,³¹ CuI, and the [Cu₂(OAc)₂]·2H₂O were obtained from commercial sources. The triethylamine used in the preparation of **8** was deoxygenated by bubbling with argon for 0.5 h directly prior to use. The alumina used for the chromatographic purification of macrocycle **5** was purchased from Merck (aluminum oxide, basic, activity I) and converted

(24) The term “twistophane” is used to describe ethynyl cyclophanes that are completely *ortho*-conjugated and helically twisted and chiral structures such as dehydrotetraarylanulenes, dehydrotetraarylanulene-type cyclophanes, and higher homologues. Cycles **1**–**5** are the first reported examples of the above type of systems with integrated heterocyclic N-donor sites for metal ion coordination.

(25) For a recent overview on fluorescent molecular sensors for cation recognition, see: Valeur, B.; Leray, I. *Coord. Chem. Rev.* **2000**, *205*, 3.

(26) For recent reviews on the preparation of coordination polymers, see: (a) Férey, G. *Chem. Mater.* **2001**, *13*, 3084. (b) Hosseini, M. Wais. In *Crystal Engineering: From Molecules and Crystals to Materials*; Braga, D., Grepioni, F., Orpen, G. A., Eds.; Kluwer: Dordrecht, 1999; pp 181–208. For the generation of a coordination polymer incorporating ethynylpyridyl-type macrocycles, see: (c) Reference 2a. For the use of curved and linear, ethynylpyridine-type ligands in the generation of coordination polymers, see: (d) Zaman, Md. B.; Smith, M. D.; zur Loye, H.-C. *Chem. Commun.* **2001**, 2256. (e) Fiscus, J. E.; Shotwell, S.; Layland, R. C.; Smith, M. D.; zur Loye, H.-C.; Bunz, U. H. F. *Chem. Commun.* **2001**, 2674. (f) Jouaiti, A.; Jullien, V.; Hosseini, M. W.; Planeix, J.-M.; De Cian, A. *Chem. Commun.* **2001**, 1114. (g) Ciurtin, D. M.; Pschirer, N. G.; Smith, M. D.; Bunz, U. H. F.; zur Loye, H.-C. *Chem. Mater.* **2001**, *13*, 2743. (h) Maekawa, M.; Konaka, H.; Suenaga, Y.; Kuroda-Sowa, T.; Munakata, M. *J. Chem. Soc., Dalton Trans.* **2000**, 4160. (i) Blake, A. J.; Champness, N. R.; Khlobystov, A.; Lemenovskii, D. A.; Li, W.-S.; Schröder, M. *Chem. Commun.* **1997**, 2027.

(27) For recent examples of metal ion-induced autoassembly of supramolecular architectures using ethynylpyridyl-type ligands, see: (a) Kawano, T.; Kato, T.; Du, C.-X.; Ueda, I. *Bull. Chem. Soc. Jpn.* **2003**, *76*, 709. (b) Kawano, T.; Kuwana, J.; Ueda, I. *Bull. Chem. Soc. Jpn.* **2003**, *76*, 789. (c) Dinolfo, P. H.; Hupp, J. T. *Chem. Mater.* **2001**, *13*, 3113. (d) Kuehl, C. J.; Huang, S. D.; Stang, P. J. *J. Am. Chem. Soc.* **2001**, *123*, 9634. (e) Justin Thomas, K. R.; Lin, J. T.; Lin, Y.-Y.; Tsai, C.; Sun, S.-S. *Organometallics* **2001**, *20*, 2262. (f) Reference 9a.

(28) The electro- and photoactive properties of structurally simple metal-complexed linear conjugated ligands have been widely studied in order to assess their potentiality for the construction of molecular level photonic devices. For reviews in this area, see: (a) De Cola, L.; Belser, P. In *Electron Transfer in Chemistry*; Balzani, V., Ed.; Wiley VCH: Weinheim, Germany, 2001; pp 97–136. (b) Barigelletti, F.; Flamigni, L. *Chem. Soc. Rev.* **2000**, *29*, 1. (c) Balzani, V.; Juris, A.; Venturi, M.; Campagna, S.; Serroni, S. *Chem. Rev.* **1996**, *96*, 759.

(29) For a report on the NLO properties of donor/acceptor substituted dehydrobenzo[18]annulenes, see: (a) Sarkar, A.; Pak, J. J.; Rayfield, G. W.; Haley, M. M. *J. Mater. Chem.* **2001**, *11*, 2943. For a recent review on the second-order NLO properties of transition-metal-complexed conjugated ligands, see: (b) Di Bella, S. *Chem. Soc. Rev.* **2001**, *30*, 355.

(30) For recent reviews on electroluminescence in metal complexes and conjugated polymers, see: (a) Kido, J.; Okamoto, Y. *Chem. Rev.* **2002**, *102*, 2357. (b) Friend, R. H.; Gymer, R. W.; Holmes, A. B.; Burroughes, J. H.; Marks, R. N.; Taliani, C.; Bradley, D. D. C.; Dos Santos, D. A.; Brédas, J. L.; Lögdlund, M.; Salaneck, W. R. *Nature* **1999**, *397*, 121.

(31) Brumbaugh, J. S.; Sen, A. *J. Am. Chem. Soc.* **1988**, *110*, 803.

(21) Literature reports on the syntheses of heterocyclic dehydroannulenes are sparse. For systems incorporating thiophene, see: (a) Boydston, A. J.; Haley, M. M.; Williams, R. V.; Armantrout, J. R. *J. Org. Chem.* **2002**, *67*, 8812. (b) Marsella, M. J.; Piao, G.; Tham, F. S. *Synthesis* **2002**, 1133. (c) Marsella, M. J.; Wang, Z.-Q.; Reid, R. J.; Yoon, K. *Org. Lett.* **2001**, *3*, 885. (d) Sarkar, A.; Haley, M. M. *Chem. Commun.* **2000**, 1733. (e) Zhang, D.; Tessier, C. A.; Youngs, W. J. *Chem. Mater.* **1999**, *11*, 3050. (f) Iyoda, M.; Vorasingha, A.; Kuwatani, Y.; Yoshida, M. *Tetrahedron Lett.* **1998**, *39*, 4701. (g) Solooki, D.; Bradshaw, J. D.; Tessier, C. A.; Youngs, W. J. *Organometallics* **1994**, *13*, 451.

(22) Conjugated polymeric scaffolds incorporating nitrogen-donor heterocycles have recently attracted considerable interest as luminescence sensors for metal ions. For examples that afford luminescence responses for Ag^I ions, see: (a) Yasuda, T.; Yamaguchi, I.; Yamamoto, T. *Adv. Mater.* **2003**, *15*, 293. (b) Bangcuoy, C. G.; Rampey-Vaughn, M. E.; Quan, L. T.; Angel, S. M.; Smith, M. D.; Bunz, U. H. F. *Macromolecules* **2002**, *35*, 1563. (c) Tong, H.; Wang, L.; Jing, X.; Wang, F. *Macromol. Rapid Commun.* **2002**, *23*, 877. (d) Tong, H.; Wang, L.; Jing, X.; Wang, F. *Macromolecules* **2002**, *35*, 7169. For recent examples of molecular luminescence sensors for Ag^I ions, see: (e) Yang, R.-H.; Chan, W.-H.; Lee, A. W. M.; Xia, P.-F.; Zhang, H.-K.; Li, K. J. *Am. Chem. Soc.* **2003**, *125*, 2884. (f) Rurack, K.; Kollmannsberger, M.; Resch-Genger, U.; Daub, J. *J. Am. Chem. Soc.* **2000**, *122*, 968. (g) Glass, T. E. *J. Am. Chem. Soc.* **2000**, *122*, 4522. (h) Wong, M. S.; Chan, W. H.; Chan, W. Y.; Li, J.; Dan, X. *Tetrahedron Lett.* **2000**, *41*, 9293.

(23) Balzani, V.; Credi, A.; Venturi, M. *ChemPhysChem* **2003**, *3*, 49.

to activity IV upon prolonged mixing with distilled water for 8 h prior to use. The silica used for all flash chromatography was also purchased from Merck (Geduran, silica gel Si 60, 40–63 μm). Intramolecular proton connectivities were determined by ^1H – ^1H COSY and NOESY NMR measurements where necessary. All ^1H and ^{13}C NMR spectra were referenced to the solvent peaks (at 6.00 and 74.0 ppm, respectively). The fluorescence and luminescence emission spectra were recorded at 20–25 °C on an Aminco, Bowman series 2 luminescence spectrophotometer (SLM Instruments, Inc.). The free ligand fluorescence emission spectra of **5**, **8**, and **9** given below were recorded in argon-bubbled CHCl_3 , and the latter two were corrected for the instrumental response. The fluorescence emission data in Table 1 were recorded in aerated solvents and were uncorrected for the instrumental response. The fluorescence spectra of **4** and **5** and the luminescence spectra of **4/Ag**⁺ and **5/Ag**⁺ in Figure 4 were recorded in 10% MeOH/ CHCl_3 and are uncorrected for the instrumental response. The luminescence emission spectra of the metal-ion-binding experiments with **5** and **8** were conducted in aerated 10% MeOH/ CHCl_3 to obtain optical responses under environmental conditions of most practical utility for sensory applications. The infrared spectrum of **5** was recorded as Nujol and polychlorotrifluoroethylene mulls; all other IR spectra were recorded as compressed KBr disks. Melting point measurements were performed in open capillaries in an apparatus calibrated with standards of known melting points. Elemental analyses were performed by the Service de Microanalyse, Institut Charles Sadron.

Thiophene-2,5-bis(2,1-ethynediyl)-bis-3-(4-trimethylsilylethynylpyridine), **8**. Toluene (35 mL), which had been freshly bubbled with argon, and **6** (1.499 g, 4.98×10^{-3} mol) were added consecutively by syringe to $\text{PdCl}_2(\text{PPh}_3)_2$ (0.078 g, 1.11×10^{-4} mol) under an atmosphere of argon. After 2 min of stirring, a solution of CuI (0.084 g, 4.41×10^{-4} mol) in Et_3N (5 mL), followed by **7** (0.327 g, 2.47×10^{-3} mol), was then added by syringe, and the mixture was stirred at ambient temperature for 5 d in the absence of light. During stirring, a dark brown suspension slowly formed. All solvent was subsequently removed under reduced pressure on a waterbath, and 20 mL of CH_2Cl_2 was added. The mixture was then chromatographed on a column of alumina (Merck, aluminum oxide 90, standardized activity II/III), eluting with CH_2Cl_2 . The glassy product thus obtained was dissolved in hexane (30 mL), Norit A decolorising charcoal (0.05 g) was added, and the mixture was stirred for 15 min. The suspension was then filtered under gravity, and the solvent was removed under reduced pressure on a waterbath. The remaining glass was dried under dynamic vacuum (0.01 mmHg) overnight, during which time it crystallized to afford **8** (0.634 g, 54%) as a yellow solid. Mp 122.6–124.6 °C. ^1H NMR ($\text{CDCl}_2\text{CDCl}_2$, 500 MHz, 20 °C): δ 8.735 (d, $^5J(2,5) = 0.6$ Hz, 2H; pyridine H2), 8.474 (d, $^3J(6,5) = 5.2$ Hz, 2H; pyridine H6), 7.390 (dd, $^3J(5,6) = 5.2$ Hz, $^5J(5,2) = 0.6$ Hz, 2H; pyridine H5), 7.284 (s, 2H; thiophene H3/4), 0.313 ppm (s, 18H; Si(CH_3)₃). ^{13}C NMR ($\text{CDCl}_2\text{CDCl}_2$, 125.8 MHz, 20 °C): δ 152.0, 148.3, 133.2, 133.0, 125.6, 124.7, 121.6, 105.8 (–C \equiv), 100.3 (–C \equiv), 90.3 (–C \equiv), 89.0 (–C \equiv), –0.05 ppm (Si(CH_3)₃). UV–vis (CH_2Cl_2): λ_{max} (ϵ) = 371 (35279), 391 (26048 $\text{M}^{-1} \text{cm}^{-1}$). Fluorescence emission (**8**) = 3.34×10^{-6} mol dm^{-3} in CHCl_3 ; 371 nm excitation): $\lambda_{\text{max}} = 407, 430$ nm. IR: 2954 (m), 2205 (m) (C \equiv C), 2161 (w) (C \equiv C), 1575 (s), 1400 (s), 1246 (s), 867 (s), 848 (s), 836 cm^{-1} (s). FAB MS (CHCl_3): m/z (%) 479 (100) [$\text{M}^+ + \text{H}$]. HRMS (FAB, CHCl_3 , [$\text{M}^+ + \text{H}$]) calcd for $\text{C}_{28}\text{H}_{27}\text{N}_2\text{SSi}_2$ 479.1434, found 479.1424. Anal. Calcd for $\text{C}_{28}\text{H}_{26}\text{N}_2\text{SSi}_2$: C, 70.24; H, 5.47; N, 5.85; S, 6.70. Found: C, 70.27; H, 5.24; N, 5.73; S, 6.56.

Thiophene-2,5-bis(2,1-ethynediyl)-bis-3-(4-ethynylpyridine), **9**. TBAF (2.8 mL, 2.80×10^{-3} mol, 1.0 M solution in THF) was added to a stirred solution of **8** (0.634 g, 1.32×10^{-3} mol) in THF (20 mL) and distilled water (0.5 mL). The yellow-brownish solution was then stirred at ambient temperature in the absence of light for 20 h. All solvent was removed under

reduced pressure on a waterbath at 20–30 °C, and distilled water (50 mL) added. The mixture was homogenized by stirring and brief ultrasonication, followed by filtration under vacuum and air-drying. The crude product was dissolved in CH_2Cl_2 and twice chromatographed on columns of alumina (Merck, aluminum oxide 90, standardized activity II/III), eluting with CH_2Cl_2 . The chromatography had to be performed in subdued light because of the enhanced photosensitivity of **9**. The product thus obtained was washed with two 4-mL portions of cold pentane, air-dried, and further dried under dynamic vacuum (0.01 mmHg) to furnish **9** (0.388 g, 88%) as a light-sensitive yellow solid. Mp 148.5–150.5 °C. ^1H NMR ($\text{CDCl}_2\text{CDCl}_2$, 500 MHz, 20 °C): δ 8.756 (s, 2H; pyridine H2), 8.512 (d, $^3J(6,5) = 5.2$ Hz, 2H; pyridine H6), 7.422 (d, $^3J(5,6) = 5.2$ Hz, 2H; pyridine H5), 7.303 (s, 2H; thiophene H3/4), 3.683 ppm (s, 2H; $\text{H}-\text{C}\equiv\text{C}$). ^{13}C NMR ($\text{CDCl}_2\text{CDCl}_2$, 125.8 MHz, 20 °C): δ 152.1, 148.5, 133.2, 132.0, 126.0, 124.7, 121.8, 90.1 (–C \equiv), 89.2 (–C \equiv), 86.8 (–C \equiv), 79.6 ppm (–C \equiv). UV–vis (CH_2Cl_2): λ_{max} (ϵ) = 367 (44945), 387 (32127 $\text{M}^{-1} \text{cm}^{-1}$). Fluorescence emission (**9**) = 4.07×10^{-6} mol dm^{-3} in CHCl_3 ; 367 nm excitation): $\lambda_{\text{max}} = 403, 425$ nm. IR: 3290 (H–C \equiv) (s), 3056 (w), 2205 (C \equiv C) (s), 2114 (C \equiv C) (w), 2097 (C \equiv C) (w), 1576 (s), 1474 (m), 1397 (s), 836 (s), 823 (s), 649 (s), 579 (m), 351 cm^{-1} (m); EI MS (CHCl_3): m/z (%) 334 (100) [M^+]. HRMS (FAB, [$\text{M}^+ + \text{H}$]) calcd for $\text{C}_{22}\text{H}_{11}\text{N}_2\text{S}$ 335.0643, found 335.0640.

Macrocycle 5. In a well-ventilated hood, $[\text{Cu}_2(\text{OAc})_4] \cdot 2\text{H}_2\text{O}$ (2.60 g, 6.51×10^{-3} mol) was dissolved in warm pyridine (650 mL), and the stirred solution was bubbled with argon for 1.5 h, during which time it cooled to ambient temperature. A solution of **9** (0.200 g, 5.98×10^{-4} mol) in toluene³² (20 mL) was then slowly added dropwise over 7 h to the $\text{Cu}_2(\text{OAc})_4$ solution, with continued stirring and argon bubbling. After the addition of **9** was complete, the reaction was stirred under a static atmosphere of argon, at ambient temperature and in the absence of light for 7 d. During the addition of **9**, the reaction changed color from blue to olive-green, and finally the development of a yellow suspended solid was complete after 48 h stirring.³³ All solvent was removed under reduced pressure on a waterbath, and pyridine (5 mL) was re-added to wet the residue, followed by distilled water (300 mL) and excess ice. Solid KCN was then added in 0.2-g portions to the rapidly stirred mixture, until no further visible change occurred, at which point it appeared as a yellow-brown suspension in a pale brown-colored solution. The suspended solid was then isolated by filtration under vacuum, washed with excess distilled water followed by MeOH to remove the brown-colored contaminants, Et_2O , and finally air-dried. The poorly soluble yellow product was dissolved in boiling CHCl_3 (800 mL) and chromatographed on a column of alumina (basic, activity IV), gradient eluting first with CHCl_3 followed by 5% MeCN/ CHCl_3 and last 10% MeCN/ CHCl_3 . Because of the enhanced photosensitivity of solutions of **9**, the chromatography and subsequent manipulations were conducted with shielding from direct light. The product thus obtained was finally briefly stirred in CH_2Cl_2 (4 mL) and filtered under vacuum, and the collected solid was washed with CH_2Cl_2 (2×2 mL) and air-dried to give **5** (0.092 g, 46%) as a light-sensitive bright-yellow powder. Mp: slow heating from 276 to 312 °C induces color darkening to give a black infusible solid. Upon rapid heating, **5** ignites explosively at ≥ 294.5 °C. ^1H NMR ($\text{CDCl}_2\text{CDCl}_2$, 500 MHz, 90 °C): δ 8.785 (s, 4H; pyridine H2), 8.591 (d, $^3J(6,5) = 5.2$ Hz, 4H; pyridine H6), 7.451 (d, $^3J(5,6) = 5.2$ Hz, 4H; pyridine H5), 7.191 ppm (s, 4H; thiophene H3/4). ^{13}C NMR ($\text{CDCl}_2\text{CDCl}_2$, 125.8 MHz, 90 °C): δ 152.0 (pyridine C2), 148.5

(32) It may be noted that solutions of **9** in pyridine and toluene are rather unstable, turning black upon standing at ambient temperature, even in the dark, for 24 h. The stability of **9** is, however, much lower in pyridine. For example, a solution of 0.20 g of **9** in 20 mL of pyridine underwent 50% decomposition at ambient temperature in the dark during 24 h, based upon recovered starting material.

(33) It is possible that this yellow precipitate is a network coordination polymer that forms upon reaction between $\text{Cu}_2(\text{OAc})_4$ and **5** as it is generated.

(pyridine C6), 133.4 (thiophene C3, 4), 131.2, 125.2 (pyridine C5), 124.8, 122.7, 90.3 (–C≡), 89.9 (–C≡), 81.4 (–C≡), 80.6 ppm (–C≡). UV–vis (CH₂Cl₂): λ_{max} (ϵ) = 292sh (53350), 310 (82698), 332 (81573), 380 (49940 M⁻¹ cm⁻¹). Fluorescence emission ([5] = 9.63 × 10⁻⁶ mol dm⁻³ in CHCl₃; 332 nm excitation): λ_{max} = 485 nm. IR: 2216 (C=C) (w), 2204 (C≡C) (s), 2143 (C≡C) (w), 1571 (s), 1406 (s), 838 (s), 822 (s), 791 (s), 573 cm⁻¹ (s). FAB MS (NBA/TFA): *m/z* (%) 665 (100) [M⁺ + H]. HRMS (FAB, NBA/TFA, [M⁺ + H]) calcd for C₄₄H₁₇N₄S₂ 665.0895, found 665.0916. The product prepared as described above afforded clean NMR and mass spectra. However, analytically pure **5** could be obtained upon dissolving the cycle in boiling CHCl₃ (400 mL), gravity filtering the solution, and removing the solvent under reduced pressure on a waterbath. The solid was then briefly boiled in MeCN (100 mL), the cooled suspension was filtered under vacuum, and the isolated solid was washed with MeCN and air-dried. The product was finally recrystallized from boiling pyridine and dried under dynamic vacuum at 0.01 mmHg. The latter recrystallization was accompanied by some product decomposition to a pyridine-

soluble brown residue. Anal. Calcd For C₄₄H₁₆N₄S₂: C, 79.50; H, 2.43; N, 8.43; S, 9.65. Found: C, 79.17; H, 2.38; N, 8.63; S, 9.78.

Acknowledgment. The Collège de France and the Institut Charles Sadron are acknowledged for financial support and Roland Graff for the ¹H NMR COSY, NOESY, ROESY, and HSQC experiments. Prof. Alexandre Varnek is also thanked for the molecular modeling studies and Dr. Marie-Thérèse Youinou for constructive comments.

Supporting Information Available: Fluorescence pH titration curves of **4** and **5** with CF₃COOH in CHCl₃ solution and ¹H and ¹³C spectra of **5** and **9**. This material is available free of charge via the Internet at <http://pubs.acs.org>.

JO0302410